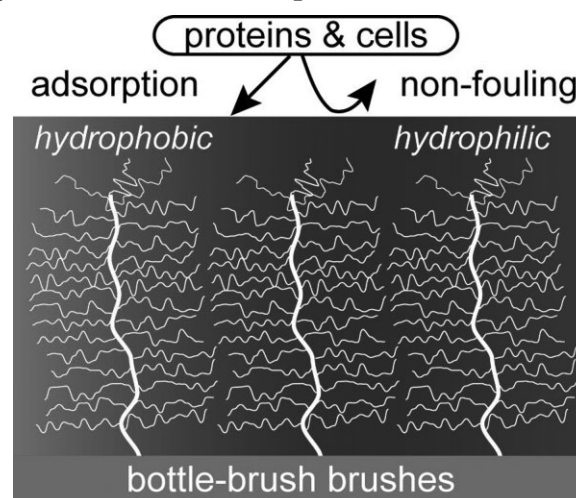


# Tailored Poly(2-oxazoline) Polymer Brushes to Control Protein Adsorption and Cell Adhesion

Ning Zhang, Tilo Pompe,\* Ihsan Amin, Robert Luxenhofer, Carsten Werner, Rainer Jordan\*

POx bottle-brush brushes (BBBs) are synthesized by SIPGP of 2-isopropenyl-2-oxazoline and consecutive LCROP of 2-oxazolines on 3-aminopropyltrimethoxysilane-modified silicon substrates. The side chain hydrophilicity and polarity are varied. The impact of the chemical composition and architecture of the BBB upon protein (fibronectin) adsorption and endothelial cell adhesion are investigated and prove extremely low protein adsorption and cell adhesion on BBBs with hydrophilic side chains such as poly(2-methyl-2-oxazoline) and poly(2-ethyl-2-oxazoline). The influence of the POx side chain terminal function upon adsorption and adhesion is minor but the side chain length has a significant effect on bioadsorption.



## 1. Introduction

The modification of surfaces to control protein adsorption and cell adhesion is a key technology for the development of

biomaterials as implants or in regenerative therapy. No general recipe for the design of protein-resistant or “non-fouling” surfaces is available, as the response of an organism towards foreign materials is highly developed and complex.<sup>[1]</sup> However, for specific applications various coating designs have been developed and research focuses on defined systems that allow the identification of a structure-property relationship. Among those, self-assembled monolayers (SAMs)<sup>[2,3]</sup> and polymer brushes are the most intensely studied systems.<sup>[4,5]</sup>

In detailed studies, the groups of Prime and Whitesides<sup>[6]</sup> and Grunze and coworkers<sup>[7,8]</sup> reported on the non-fouling properties of oligo(ethylene glycol)-terminated SAMs (OEG-SAMs) on metals and since then, OEG and longer poly-(ethylene glycol) (PEG) brush surface coatings became the gold standard for “bioinert” model surfaces. Later on, several research groups<sup>[9–13]</sup> introduced highly crowded bottle-brush brushes (BBBs) of acrylates featuring OEG as defined side chains as protein resistant surfaces. An analog approach was then employed by Ionov et al.<sup>[14]</sup> using copoly(methacrylates) bearing pendant 2-aminoethyl

N. Zhang, R. Jordan

Wacker-Lehrstuhl für Makromolekulare Chemie, Chemie-Department, TU München, Lichtenbergstr. 4, 85748 Garching, Germany

E-mail: Rainer.Jordan@tu-dresden.de

T. Pompe, C. Werner

Max Bergmann Center of Biomaterials, Leibniz Institute of Polymer Research Dresden, 01069 Dresden, Germany

E-mail: tilo.pompe@uni-leipzig.de

T. Pompe

Current Address: Institute of Biochemistry, Universität Leipzig, Johannisallee 21, 04103 Leipzig, Germany

I. Amin, R. Luxenhofer, R. Jordan

Lehrstuhl für Makromolekulare Chemie, Chemie-Department, TU Dresden, Zellescher Weg 19, 01069 Dresden, Germany

C. Werner, R. Jordan

Center for Regenerative Therapies Dresden, Dresden, Germany

hydrochloride functions for strong adhesion of the copolymer on glass and OEG-side chains to suppress unspecific kinesin-1 adsorption. Later, the same group presented BBBs prepared by surface-initiated controlled radical polymerization (SI-ATRP) with a poly(*N*-isopropylacrylamide) (PNIPAAm) backbone and OEG side chains with switchable adhesion properties. Very recently, the groups of Huck and coworkers<sup>[15]</sup> reported on the protein repellent properties of polyacrylate brushes prepared by SI-ATRP. Using acrylate monomers with pendant glycerol, linear oligoglycerol and dendronized glycerol groups, they presented a study of the impact of the effect of polymer brush architecture on the protein repellent properties using various proteins [fibronectin (Fn), albumin], human blood plasma, and serum. According to the earlier findings,<sup>[9–13,16,17]</sup> lowest adsorption was found for the bottle-brush architecture featuring oligomeric side chains. The effect of hydrophilic and flexible polymer side chains is believed to result from intermolecular interactions based on steric repulsions and entropic chain flexibility.<sup>[18–20]</sup>

While PEG is now the most widely used polymer for “biocompatibilization” of solids, poly(2-oxazoline)s (POx) are currently entering the field of biomaterials.<sup>[21–30]</sup> Especially the water-soluble poly(2-methyl-2-oxazoline) (PMeOx) and poly(2-ethyl-2-oxazoline) (PEtOx) were found to prolong the blood circulation time of liposomes when incorporated as lipopolymers for stabilization.<sup>[31–34]</sup> POx-based lipopolymers<sup>[35]</sup> are used successfully for the construction of biomimetic cell membranes on solids<sup>[36–39]</sup> and the low interaction with proteins allows for transmembrane protein integration<sup>[40]</sup> and quantitative studies of integrin-mediated cell binding experiments.<sup>[41–43]</sup> While PMeOx is highly hydrophilic, PEtOx is still well water soluble but shows a slight amphiphilicity, similar to PEG.<sup>[44,45]</sup> As a polyether, PEG coatings may lose their function in complex biological fluids or in salt water media and can undergo oxidative degradation leading to chain scission as well as oxidation of chain termini (PEG poisoning)<sup>[46]</sup> when used for longer time.<sup>[47,48]</sup> In contrast to this, the tertiary amide group of POx as well as its polysoap structure (amphiphilicity of each monomer unit) might be advantageous. Already in early studies, Lehmann and R  he et al.<sup>[49]</sup> reported first results on PEtOx brushes on gold that significantly reduce the adsorption of Fn and recently, Yan and coworkers<sup>[50]</sup> showed significant reduction of lectin adsorption on photografted PEtOx films. In a conclusive study, Textor et al.<sup>[16,17]</sup> presented adsorbed layers of poly(L-lysine) (PLL)/PMeOx bottle-brushes as highly effective protein repellent surfaces. All present studies indicate that hydrophilic POx is non-cytotoxic,<sup>[29,51]</sup> of low acute toxicity<sup>[25]</sup> and in contrast to PEG not accumulated in a specific organ but rapidly cleared from the blood pool in its free form.<sup>[52]</sup>

While several systems demonstrated the protein-repellent properties of POx equal to PEG systems, a long-term in-body application of POx-coated substrates such as implants or sensors calls for a stable coating via covalent bonding, ideally in a brush morphology. Especially, the BBBs with OEG or PEG side chains are intriguing as the critical polymer chain length to obtain protein repellency is relatively low,<sup>[6,53]</sup> however, chain crowding is crucial.<sup>[18,19]</sup> A closer look at biological systems seems to confirm that the BBB motif seems to be most suitable to regulate protein adsorption and to control cell/surface interactions: the same architectural motif of BBBs (and very similar molecular morphology)<sup>[54]</sup> is shared by proteoglycans. Proteoglycans are a major component of the extracellular matrix and can also be found on the cell surface of adhered cells. Among their multiple and very diverse functions, they play a significant role in cell adhesion, motility, proliferation, stem cell differentiation, and tissue morphogenesis and later determine the mechanical strength of tissue.<sup>[55–58]</sup>

POx-based comb polymers or, for high side chain grafting densities, bottle-brush structures (also referred to as molecular brushes or cylindrical brushes) can be realized by, e.g., the “grafting through,”<sup>[59,60]</sup> “grafting onto,” or “grafting from”<sup>[61,62]</sup> approach. For surfaces, the grafting from or surface-initiated polymerization is most advantageous in order to realize high grafting densities with respect to stem and side chain grafting. Recently, we reported on the preparation of POx-based BBBs via a two-step polymerization.<sup>[63]</sup> First, the BBB backbone is formed by living anionic or free-radical polymerization of 2-isopropenyl-2-oxazoline (IPOx), followed by the grafting-from reaction to build the BBB side chains by living cationic ring-opening polymerization (LCROP) of various 2-oxazolines including MeOx and EtOx. As the second polymerization used a charged macroinitiator, the side chain grafting efficiency is nearly quantitative and thus results in BBBs of high side chain crowding.<sup>[62]</sup> This concept could be readily used to prepare grafted BBBs of different compositions and on various surfaces. Here, the BBB stem was grafted by means of self-initiated photografting and photopolymerization (SIPGP) directly on glassy carbon<sup>[63]</sup> or diamond<sup>[64,65]</sup> as both substrates are suitable for biosensing. Moreover, the BBB architecture and the POx chemistry allows for multiple functionalizations at the side chain pendant and terminal positions. Hole transporting groups (carbazole)<sup>[64]</sup> as well as large model proteins (e.g., GFP)<sup>[65]</sup> have been introduced and demonstrating the versatility of the system for biosensing purposes. However, as glassy carbon and especially diamond shows already exceptional biocompatibility<sup>[66]</sup> the protein repellent properties of the POx-BBB coatings were not addressed. In this study we prepared analog POx-BBB systems on amino-functionalized silicon/silicon dioxide substrates to evaluate the effect of BBB coating as a function of POx-BBB side chain

composition, length, and end function. Glass substrates are notoriously problematic in terms of unspecific protein adsorption and cell adhesion. Moreover, surface amino groups are known to significantly promote protein adhesion and cell growth/adhesion and thus, the “non-fouling” properties of various POx-BBBs grafted on such surfaces will give conclusive results. For the facile preparation of stable polymer grafts, we took advantage of the preferred grafting via SIPGP onto the amino functionalized SAMs.<sup>[67,68]</sup> The aim of this study was to screen the regulation of protein adsorption and successive cell adhesion by the structural and compositional variation of surface grafted BBBs.

## 2. Experimental Section

### 2.1. Materials

All substances were purchased from Sigma-Aldrich (Steinheim, Germany) or Acros (Geel, Belgium) and used as received unless otherwise stated. Methyl triflate (MeOTf), 2-methyl-2-oxazoline (MeOx), 2-ethyl-2-oxazoline (EtOx), 2-*n*-propyl-2-oxazoline (*n*PrOx), IPOx, and acetonitrile (ACN) were dried by refluxing over CaH<sub>2</sub> under a dry nitrogen atmosphere and were subsequently distilled prior to use. Silicon (100) wafers with a natural oxidized layer were received as a gift from Wacker-Siltronic GmbH (Germany).

Infrared spectroscopy (IR) was performed using an IFS 55 Bruker instrument equipped with a diffuse-reflectance Fourier-transform infrared (DRIFT) setup from SpectraTech and a mercury/cadmium telluride (MCT) detector. For each spectrum, 500 scans were accumulated with a spectral resolution of 4 cm<sup>-1</sup>. Background spectra were recorded on bare oxidized silicon substrates.

Atomic force microscopy (AFM) was performed on a Nano-scope IIIa scanning probe microscope from Veeco Instruments (Mannheim, Germany). The microscope was operated in tapping mode using Si cantilevers with a resonance frequency of 273 kHz, a driving amplitude of 1.30 V at a scan rate of 0.3 Hz. Layer thickness of grafted brushes were determined by measuring step height of small scratches in the polymer layer.

### 2.2. Contact Angle (CA)

The water contact angles were determined with a fully automated Krüss DSA 10 Mk2 contact angle goniometer. Given contact angle values and errors were calculated from three measurements on three different areas on each surface. The data were obtained with the aid of the Krüss Drop Shape Analysis v3 software package.

2-Isopropenyl-2-oxazoline and *n*PrOx were synthesized according to procedure published previously.<sup>[69,70]</sup> *n*PrOx: in a Schlenk flask, 15 g (0.21 mol, 1.0 equiv.) of butyronitrile, 18 g (0.26 mol, 1.2 equiv.) aminoethanol and 0.9 g (3.2 mmol) cadmium acetate dihydrate were stirred and heated to 130 °C. After 12 h, the reaction was cooled to room temperature (RT). The red raw product was purified by vacuum distillation and stored under a dry nitrogen atmosphere prior to use (yield, 16.5 g, 68%). <sup>1</sup>H NMR (250 MHz, CDCl<sub>3</sub>, δ): 4.27 (t, 2H), 3.81 (t, 2H), 2.23 (t, 2H), 1.69 (st, 2H), 0.95 (t, 3H).

For IPOx: 2-ethyl-oxazoline reacted with 1 equiv. of paraformaldehyde in the presence of catalytic amounts of triethylamine to form the hydroxyethyl derivative. Water was eliminated at elevated temperatures when alkali metal alkoxide is used as catalysts. Finally, 2-isopropenyl-oxazoline was distilled under reduced pressure before use. <sup>1</sup>H NMR (250 MHz, CDCl<sub>3</sub>, δ): 5.78 (s, 1H), 5.41 (s, 1H), 4.27 (t, 2H), 3.93 (t, 2H), 2.00 (t, 3H).

### 2.3. α,ω-Aminopropyltrimethoxysilane Monolayer

A substrate was first cleaned by piranha solution (H<sub>2</sub>SO<sub>4</sub>/H<sub>2</sub>O<sub>2</sub> = 3/1, attention!) and successively rinsed with freshly deionized water (Millipore) to neutrality. The substrates were submerged in a 5 vol% 3-aminopropyltrimethoxysilane solution in dry acetone and ultrasonicated for 30 min at room temperature (RT) under a dry nitrogen atmosphere. Finally, the substrates were rinsed with dry acetone (HPLC-grade) and then dried under vacuum.

### 2.4. IPOx Polymer Brushes: SIPGP

According to our reported procedure for the preparation of BBBs of 2-oxazolines on glassy carbon,<sup>[63]</sup> a substrate coated with a α,ω-aminopropyltrimethoxysilane monolayer was submerged in approximately 5 mL of freshly distilled and degassed IPOx in a Duran glass vial. Polymerization was allowed to complete in 24 h under constant irradiation with UV light at λ<sub>max</sub> = 350 nm at RT. Immediately after photopolymerization, the samples were cleaned by sequential ultrasonication in ethanol, ethyl acetate and toluene (all HPLC-grade) for 1 min each.

### 2.5. BBBs: SI-LCROP

#### 2.5.1. Variation of Side-Chain End Groups (PMeOx-Boc, PMeOx-Pip, PMeOx-OH, PMeOx-E)

A PIPOx brush modified substrate was submerged in a solution of 2 mL ACN with an excess amount of MeOTf (30 mg) at approximately -35 °C under a dry argon atmosphere. After stirring for 5 h at 0–5 °C, the mixture was allowed to equilibrate to RT and stirred for 1 h. To the reaction vial, 1 g MeOx was added. The reaction solution was heated at 80 °C and stirred for 4 h. Then, the solution was cooled to 0 °C, and an excess of terminating agent dissolved in 1 mL of ACN was added under argon atmosphere and the solution was stirred for 16 h at RT. Afterwards, an excess of potassium carbonate was added to the solution and stirred overnight. The substrate was removed from the reaction solution and cleaned by sequential ultrasonication in deionized water, ethanol, and ethyl acetate for 1 min each.

To ensure comparability of the substrates with variation of only the side chain end group of the BBB, one longer substrate was used for monolayer preparation and PIPOx brush growth. The long substrate was then cut into four pieces and SI-LCROP of MeOx was performed under identical conditions but variation of the terminating agent: *N*-Boc-piperazine for PMeOx-Boc, piperidine for PMeOx-Pip, 4-piperidinol for PMeOx-OH, and ethyl isonipicotate for PMeOx-E. After the thorough cleaning procedure, the resulting polymer layer thickness was determined by AFM. For instance, after 4 h SI-LCROP of MeOx and piperidine capping, the

polymer layer thickness increased by 128% from  $56 \pm 3$  nm for the PIPOx brush to  $140 \pm 10$  nm for PMeOx-Pip.

### 2.5.2. Variation of Side-Chain Composition (PMeOx, PEtOx, PnPrOx)

According to the above-described procedure, a longer substrate with PIPOx brush was divided into three pieces and SI-LCROP was performed with MeOx, EtOx, and *n*PrOx as the monomers and piperidine as the terminating agent. The polymer-coated substrates were thoroughly cleaned by ultrasonication in water, ethanol, ethyl acetate, and toluene.

### 2.5.3. Variation of Side-Chain Length (PMeOx1-4)

According to the above-described procedure, a longer substrate with PIPOx brush was divided into three pieces and SI-LCROP were performed with MeOx as the monomer and piperidine as the terminating agent, for 1 (PMeOx1), 2 (PMeOx2), and 4 h (PMeOx4), respectively.

### 2.5.4. Variation of Substrate: BBB on Glassy Carbon

Following our previous report,<sup>[63]</sup> a BBB was prepared on freshly polished glassy carbon by SIPGP of IPOx (24 h) and SI-LCROP for 2 and 4 h at 80 °C using MeOx as the monomer and piperidine as the terminating agent.

## 2.6. Protein Adsorption and Cell Adhesion Studies

Protein adsorption and cell culture was performed similarly to procedures described recently.<sup>[71,72]</sup> Briefly, samples were immersed in 70% ethanol/water to provide sterile conditions for cell culture. Thereafter, polymer surfaces were immersed in a  $50 \mu\text{g} \cdot \text{mL}^{-1}$  Fn (purified from human plasma) solution in phosphate-buffered saline (PBS, Sigma) at pH = 7.4 and 37 °C for 1 h and subsequently rinsed twice with PBS buffer to remove weakly adsorbed Fn. Carboxytetramethylrhodamine Fluoreporter (Invitrogen, Karlsruhe, Germany) was used to label Fn prior to the experiments. The mean labeling degrees were around three fluorophores per Fn dimer.

Human endothelial cells from the umbilical cord vein (HUVECs) were seeded in endothelial cell growth medium (ECGM, Promocell, Heidelberg, Germany) containing 2% fetal calf serum at density of  $10^5$  cells per  $\text{cm}^2$  on the Fn-coated substrates and cultivated up to 24 h after seeding and investigated on an inverted light microscope in phase contrast using a  $10\times$  objective. After 1 or 3 h of cell culture some samples were fixed with 4% paraformaldehyde for 10 min and stained with 4',6-diamidino-2-phenylindole (DAPI, Sigma) and phalloidin-Alexa488 (Invitrogen) to visualize nuclei and actin cytoskeleton, respectively, in fluorescence microscopy using an inverse epi-fluorescence microscope (DMIRE2, Leica Microsystems, Germany) with a  $40\times$  oil-immersion objective. The amount of labeled Fn remaining on the substrate surface after 1 h of cell culture was analyzed in terms of fluorescence intensities using Openlab software (Perkin-Elmer). For quantification, reference intensities were collected from Fn-coated poly[octadecan-*alt*-(maleic anhydride)] (POMA) surfaces with known Fn adsorption characteristics.<sup>[72]</sup> This approach was shown recently to provide good quantitative results.<sup>[71]</sup>

## 3. Results and Discussion

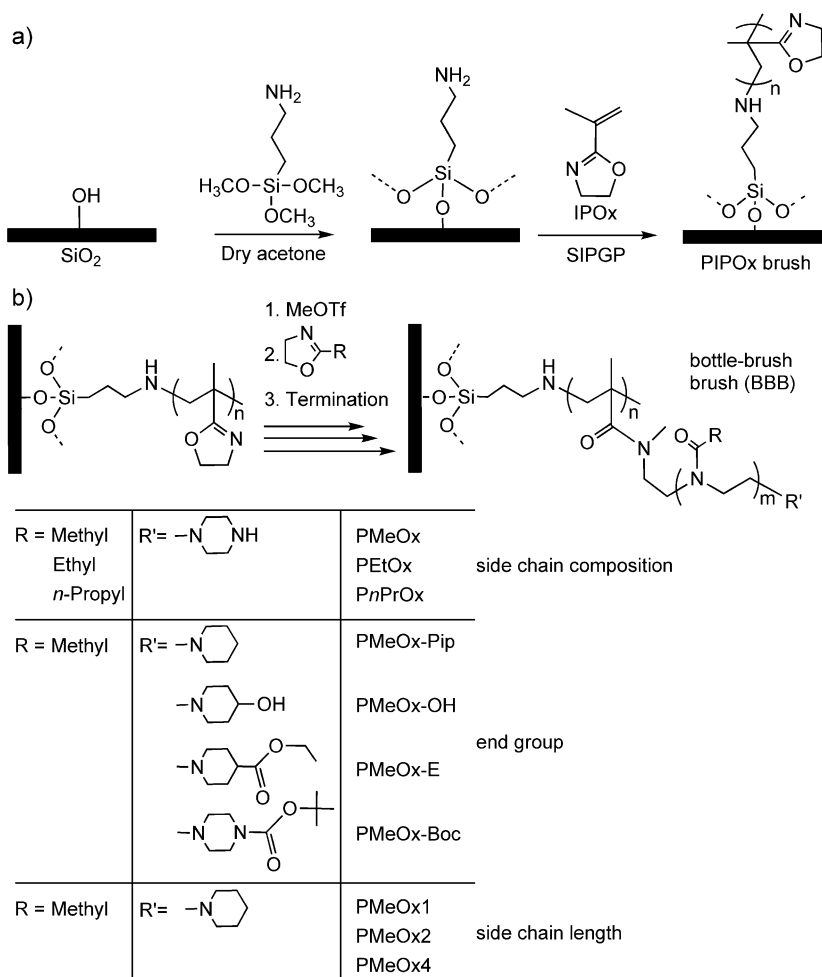
### 3.1. Synthesis and Polymer Layer Characterization

As SIPGP does not result in polymer grafting directly on silica surfaces because of the high bond dissociation energy of the surface silanol groups,<sup>[73]</sup> a SAM of  $\alpha,\omega$ -aminopropyltrimethoxysilane (APTMS) was used as the primary layer. The terminal amino function is most suitable for this purpose since it catalyses the silanization reaction and it is the most effective surface function for the SIPGP due to the low bond dissociation energy of the N–H bond.<sup>[68]</sup> The uniformity and thickness of the APTMS-SAMs were checked by X-ray photoelectron spectroscopy ( $d = 0.72$  nm) and water contact angle measurements ( $\theta = 55 \pm 3^\circ$ ) and were found in good agreement with the reported values.<sup>[74–77]</sup> Here, it is noteworthy that silanization with APTMS is not trivial as polycondensation and successive chemisorption results easily in rough and undefined films. Silanization under constant ultrasonication and good control of the water content during the silanization effectively prevent APTMS multilayer formation and homogeneous uniform monolayers were obtained.

Analog to our previous reports,<sup>[63–65]</sup> POx-based BBBs (POx-BBBs) on ATMS-SAMs were prepared by a two-step polymerization of (a) SIPGP of IPOx to PIPOx brushes and (b) SI-LCROP of MeOx, EtOx, and *n*PrOx from surface bond macroinitiator brushes. The general reaction is outlined in Scheme 1.

For all POx-BBBs, the SIPGP was performed on APTMS-SAMs submerged in bulk IPOx monomer and constant UV-irradiation for 24 h using a UV-lamp with a spectral distribution between 300 and 400 nm ( $\lambda_{\text{max}} = 350$  nm). The different side chain grafting reaction by SI-LCROP was performed on fractions of the same substrates modified by PIPOx brushes to give the best comparability. Separate substrate pieces were used to characterize the PIPOx brushes and POx-BBBs by AFM, water contact angle measurements and FTIR spectroscopy. As an example, the AFM analysis of an intentionally scratched PIPOx brush and the consecutively prepared POx-BBB with MeOx side chains and piperidine end groups (PMeOx-Pip) are shown in Figure 1.

SIPGP results in a homogeneous  $56 \pm 3$  nm thick PIPOx brush. The consecutive SI-LCROP for 4 h at 80 °C resulted in a significant thickness increase to  $140 \pm 10$  nm because of the stretching of the bottle-brush backbone by the side chain crowding.<sup>[63,65]</sup> The water contact angle values slightly decreased from  $49 \pm 2^\circ$  (PIPOx) to  $44 \pm 2^\circ$  (PMeOx-Pip). The layer thicknesses and wettability for all other samples are summarized in Table 1. The two-step polymerization was further followed by FTIR spectroscopy. Figure 2 shows the spectra of the same PIPOx (Figure 2a) and PMeOx-Pip (Figure 2b) surface. The characteristic FTIR spectra of PIPOx



**Scheme 1.** Preparation of POx-BBBs on silicon dioxide substrates. (a) Formation of self-assembled monolayer of APTMS and subsequent growth of PIPOx brushes by SI-LCROP by UV-irradiation at  $\lambda_{\max} = 350$  nm in bulk IPOx. (b) Conversion of the PIPOx brush backbone to the macroinitiator salt with methyltriflate and subsequent LCROP of 2-alkyl-2-oxazolines from the macroinitiator brush. The LCROP was quantitatively terminated by different reagents to give POx-BBBs with a systematical variation of side chain composition, side chain length, and end functions. Use of parts of a single, identically modified substrate allows comparability of different samples. In a separate series, POx-BBBs analog to PMeOx2 and PMeOx4 were prepared directly on glassy carbon substrates according to ref.<sup>[63]</sup>

brush feature strong bands at 1656 and 1130  $\text{cm}^{-1}$  assigned to the (C=N) and (C=O) stretching modes as well as the two modes at 990 and 953  $\text{cm}^{-1}$  originate from the ring skeletal vibration of the 2-oxazoline rings.<sup>[63]</sup> After SI-LCROP, these bands are no longer observable and a new intensive band appeared around 1627  $\text{cm}^{-1}$  which is characteristic for the carbonyl stretching mode of the amide function (amide I band) of POx.<sup>[35]</sup> Moreover, the characteristic  $\text{CH}_x$  deformation modes for PMeOx-Pip are observed around 1421  $\text{cm}^{-1}$ . The significant thickness increase along with the spectroscopy results are in agreement with our earlier reports and strongly indicate a quantitative conversion of the pendant 2-oxazoline rings and the formation of BBBs with densely grafted POx side chains.

Analog to PMeOx-Pip all other POx-BBB modified substrates were prepared and characterized. The analytical

results, preparation details and abbreviations for all samples are summarized in Table 1. In all cases the PIPOx preparation was kept constant. First, a variation of the BBB side chain composition was realized by dividing a long PIPOx modified substrate into three pieces and SI-LCROP with MeOx, EtOx and *n*PrOx was performed for 4 h using piperazine as the terminating agent. This results in a series of POx-BBBs (PMeOx, PEtOx, and P*n*PrOx) with side chains of increasing hydrophobicity<sup>[30]</sup> but comparable stem and side chain length. The measured water contact angles slightly increase accordingly from  $38 \pm 3^\circ$  for the very hydrophilic PMeOx,  $43^\circ$  for PEtOx to  $56 \pm 3^\circ$  for P*n*PrOx. The resulting layer thicknesses do not differ significantly as the side chain length is constant, however, the slight increase nicely reflects the increasing molar mass of the used monomer.

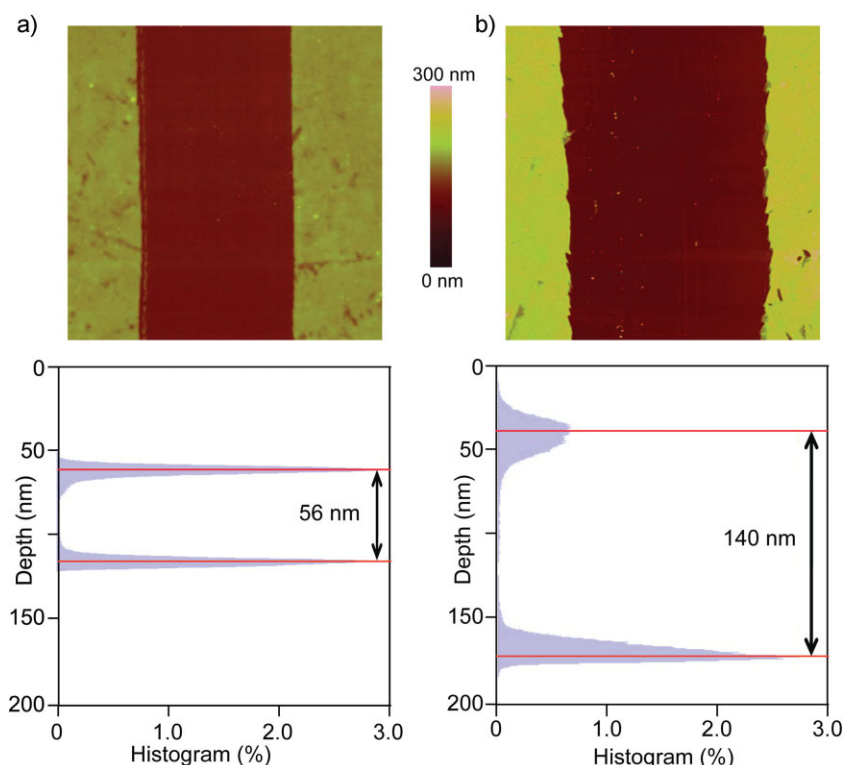


**Figure 1.** AFM scans ( $55 \times 55 \mu\text{m}^2$ ) and depth analysis of the polymer brushes. (a) The SIPGP of IPOx for 24 h at  $\lambda_{\text{max}} = 350 \text{ nm}$  results in, e.g., a  $56 \pm 3 \text{ nm}$  thick PIPOx brush. (b) The consecutive LCROP (4 h) with 2-methyl-2-oxazoline and termination gave a  $140 \pm 10 \text{ nm}$  thick BBBs. (The dark area is the bare substrate, polymer brush was removed by scratching using a sharp steel needle). Further AFM inspection of the surfaces revealed homogeneous coverage of the entire substrate and low surface roughness.

Similarly, the BBB side chain length was varied by increase of the SI-LCROP time. As SI-LCROP is a living polymerization and the polymerization was performed in an excess of monomer, the development of the chain length is linear with the polymerization time.<sup>[78]</sup> Again one PIPOx sample was divided into three pieces and SI-LCROP was performed for 1, 2, and 4 h using MeOx to result in hydrophilic BBB coatings (PMeOx1-4). The relative increase of layer thickness was found to be a linear function of the SI-LCROP polymerization time, which is in good agreement with early reports.<sup>[63]</sup> As a direct determination of the side chain length (degree of polymerization,  $n$ ) and dispersity of the BBBs is impossible, but the living cationic polymerization proceeds efficiently as a surface-initiated polymerization<sup>[78,79]</sup> as well as no indication of restricted initiation or polymerization because of crowding can be expected,<sup>[63,80]</sup> the side chain length can be estimated from the polymerization constant of the monomer considering the reaction conditions (concentration, solvent, and temperature). For PMeOx1-4 this calculates to an average side chain length of  $m = 6$  for PMeOx1,  $m = 12$  for PMeOx2 and  $m = 18$  for

PMeOx4. This estimation is in good agreement with the measured relative layer thickness increase upon SI-LCROP (Table 1). Only for a short polymerization time of 1 h the contact angle of BBBs varied significantly with the side chain length ( $51^\circ$  for PMeOx1;  $43^\circ$  for PMeOx4) indicating for these short times still a major impact of the PIPOx brush.

Finally, the side chain end group was varied while keeping stem and side chain length constant, by termination of the SI-LCROP with *N*-Boc-piperazine (PMeOx-Boc), piperidine (PMeOx-Pip), piperidinol (PMeOx-OH), and ethyl isonipecotate (PMeOx-E). Contact angles for BBBs with PMeOx side chain (LCROP = 4 h) and different end groups showed only minor changes of the contact angles. This is expected as the end functions are attached to flexible hydrophilic PMeOx chains and can undergo surface reconstruction to decrease the surface free energy upon water contact. However, the situation might be different for the interaction of BBBs with amphiphilic, strongly adsorbing proteins such as Fn.

### 3.2. Protein Adsorption and Cell Adhesion

From previous studies<sup>[16,17]</sup> PMePOx BBBs were expected to exhibit excellent protein-repellent properties. We therefore set off only to screen protein adsorption and cell adhesion behavior in respect to the large range of POx side chain parameters without an in-depth analysis of long-term protein resistance. The protein adsorption onto POx-BBBs was tested only with one fluorescently labeled protein, namely Fn, as it can be used as a good reference in non-specific protein adsorption due to its large size and high conformational flexibility making it prone to adsorb at various surfaces. In that sense it performs similarly well to other proteins such as fibrinogen which is frequently used in protein adsorption studies. Furthermore, its existence provides excellent cell adhesion by its ligands (e.g., RGD sequence) for cell surface integrins even at low surface coverage making cell adhesion studies quite sensitive for Fn adsorption. As more protein adsorption was studied in combination with cell adhesion using serum containing media up to 24 h of cell culture, the cell adhesion studies provided a further indirect proof of protein adsorption from more complex and more concentrated protein solutions.

Table 1. Summary of the synthesis and surface characteristics for BBBs of 2-oxazolines on silicon dioxide and glassy carbon.

Sample	Monomer	Reaction time [h]	Terminating agent	PIPOx brush		BBB	
				$\theta^a)$ [°]	$d^b)$ [nm]	$\theta^a)$ [°]	$d^b)$ [nm]
PMeOx	MeOx	5	piperazine	51 ± 2	67 ± 8	38 ± 3	245 ± 7
PEtOx	EtOx	5			73 ± 9	43	260 ± 11
PnPrOx	nPrOx	5			78 ± 9	56 ± 3	267 ± 10
PMeOx1	MeOx	1	piperidine	50 ± 2	42 ± 6	51 ± 2	62 ± 7
PMeOx2	MeOx	2			51 ± 7	45 ± 2	82 ± 6
PMeOx4	MeOx	4			50 ± 6	43 ± 2	116 ± 5
PMeOx2 <sup>GC</sup>	MeOx	2		51 ± 2	55 ± 3	42 ± 2	133 ± 4
PMeOx4 <sup>GC</sup>	MeOx	4			55 ± 3	43 ± 2	142 ± 3
PMeOx-Boc	MeOx	4	N-Boc-piperazine	49 ± 2	49 ± 5	46 ± 2	101 ± 6
PMeOx-Pip			piperidine		56 ± 3	44 ± 2	140 ± 10
PMeOx-OH			4-piperidinol		54 ± 5	33 ± 2	117 ± 7
PMeOx-E			ethyl isonipecotate		51 ± 6	42 ± 2	110 ± 5

<sup>a)</sup>Static water contact angle (mean value from at least three independent measurements); <sup>b)</sup>Polymer brush thickness determined under ambient conditions by AFM depth analysis on separate substrate fractions as shown in Figure 1; as POx is hygroscopic the layer is partially swollen by ambient humidity but not fully hydrated.<sup>[44]</sup>

In our studies non-adsorbed Fn was removed by rinsing twice with PBS buffer prior cell adhesion studies in serum-containing medium. Fluorescence microscopic analysis was used to quantify Fn adsorption on all

surfaces based on our good experience with such assays in earlier studies.<sup>[71]</sup> Figure 3 shows the fluorescent images of the POx-BBBs with a variation of side chain composition PnPrOx, PEtOx, and PMeOx after the Fn adsorption and incubation in cell culture medium for 1 h.

Strong fluorescence originating from adsorbed stained Fn could be detected on PnPrOx with its more hydrophobic side chains. Please note that the Fn adsorption was performed at 37 °C, and thus above the cloud point of the PnPrOx homopolymer<sup>[70,81–83]</sup> with this specific end group<sup>[84]</sup> and very recently, we determined the cloud point for the PIPOx-*g*-PnPrOx molecular brush polymer in aqueous solution to be 18–20 °C.<sup>[85]</sup> Almost no fluorescence signal was found on the more hydrophilic PEtOx and PMeOx. For the variation of MeOx side chain length we observed an increased fluorescence for the shortest MeOx side chain (PMOx1) in comparison to the longer side chains of PMOx2 and PMOx4 with an effective suppression of Fn adsorption (data not shown). The Fn adsorption was quantified using the fluorescence intensity per unit area relative to a reference surface of POMA with a known amount (600 ng · cm<sup>-2</sup>) of Fn specifically chemisorbed to POMA via stable amide bonds.<sup>[72,86]</sup> This approach is known to provide good quantitative estimated of protein adsorption.<sup>[71]</sup> The quantitative analysis is summarized in Figure 4.

The relatively high Fn adsorption for PnPrOx surfaces can be estimated to 90 ng · cm<sup>-2</sup>. The adsorption onto PEtOx is strongly reduced and comparable to the most hydrophilic

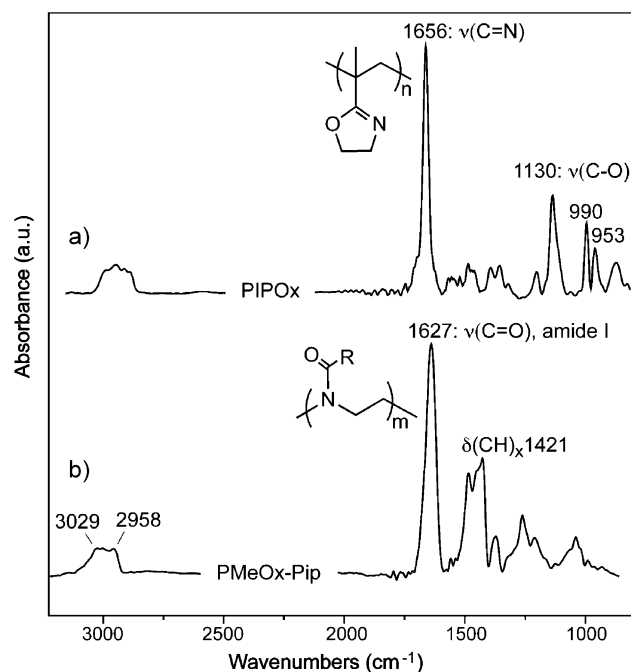
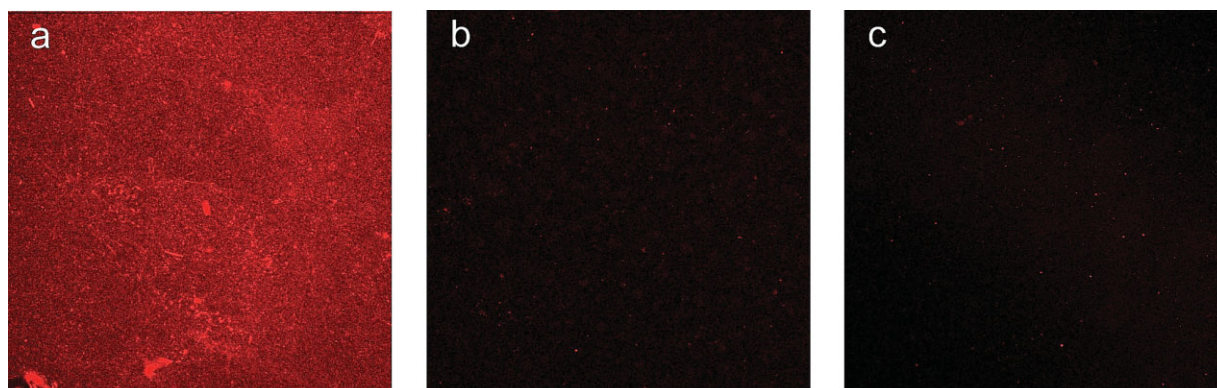
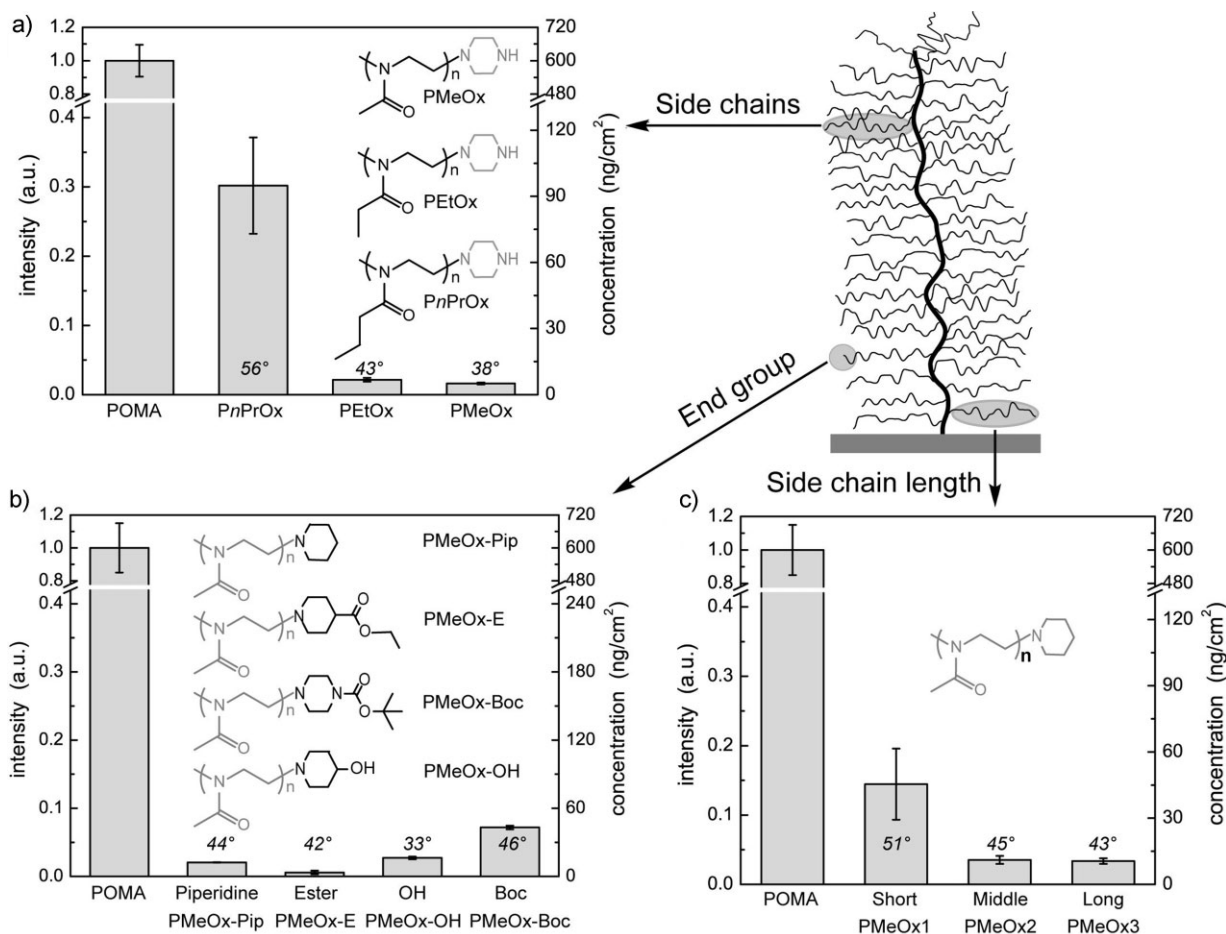


Figure 2. FTIR spectra of (a) a PIPOx brush after SIPGP (24 h) and (b) PMeOx-Pip bottle-brush brush after LCROP (4 h) and termination.



**Figure 3.** Fluorescence microscopy of Fn adsorption on grafted POx-BBBs on glass with different side composition: (a) PnPrOx, (b) PEtOx, and (c) PMeOx. Fn adsorption was performed for 1 h in a  $50 \mu\text{g} \cdot \text{mL}^{-1}$  solution of labeled Fn in PBS at pH = 7.4 and  $37^\circ\text{C}$ .



**Figure 4.** Relative intensity and absolute amount of Fn adsorption on poly(2-oxazoline) BBBs as a function of BBB architecture and composition. (a) BBBs with PMeOx, PEtOx, and PnPrOx side chains. All POx-BBBs with identical stem and approximately same side chain length. (b) BBBs with PMeOx side chain of identical side chain and stem length but variation of the side chain end group. (c) BBBs of identical stem length and PMeOx side chain of different length. The amount of adsorbed Fn was determined from fluorescence intensity after 1 h of cell culture. From the reference (Fn covalently bound to POMA layers), an estimate of absolute Fn surface concentration per unit area can be calculated.<sup>[72]</sup> The respective water contact angles are given in italics.

PMeOx surface with  $\leq 6 \text{ ng} \cdot \text{cm}^{-2}$  adsorbed Fn (near to the detection limit around  $1 \text{ ng} \cdot \text{cm}^{-2}$ ). This value is in the same low range of some  $\text{ng} \cdot \text{cm}^{-2}$  as reported for the adsorbed PLL-PMeOx BBB<sup>[16]</sup> and the surface grafted BBBs featuring OEG<sup>[9]</sup> and oligoglycerol<sup>[15]</sup> side chains indicating a similar performance in protein repellency of our PMeOX BBB. Interestingly, the PMeOx side chain length had a significant influence on the amount of Fn adsorption. While on the PMeOx1 with very short side chains  $\approx 45 \text{ ng} \cdot \text{cm}^{-2}$  Fn was found, only  $\leq 11 \text{ ng} \cdot \text{cm}^{-2}$  Fn was calculated for PMeOx4 with long pendant chains indicating a heterogeneous surface for BBBs equipped with short side chains. The nature and polarity of the side chain end groups upon the Fn adsorption had some, but compared to the other structural and compositional parameters only a slight effect (Figure 4b). For PMeOx-Pip, PMeOx-E low Fn adsorption was observed and the slightly higher Fn adsorption for PMeOx-Boc this is expectable because of the higher contact angle value due to the terminal *tert*-butyl moiety. Interestingly, for the most hydrophilic surface, PMeOx-OH, bearing a terminal hydroxyl group a higher Fn adsorption was measured as compared to PMeOx-E equipped with an ester function. This is in agreement with the findings by Whitesides and coworkers<sup>[3]</sup> who reported that especially hydrogen-bonding donors increase protein adsorption even though water contact angles are low. However, their studies were performed with SAMs and thus, a direct comparison of the results obtained with quite rigid monolayers with our findings with a highly mobile polymer brush surface have to be taken with great caution.

Finally, we performed Fn adsorption experiments on the POx-BBB grafted directly on glassy carbon to elucidate the influence of the underlying substrate. Both samples, PMeOx2<sup>GC</sup> and PMeOx4<sup>GC</sup> were prepared analog to PMeOx2 and PMeOx4 as reported previously<sup>[63]</sup> and resulted in comparable surface properties in terms of wettability and polymer brush layer thickness (Table 1). The Fn adsorption behavior on both surfaces was found to be similarly low ( $\leq 6 \text{ ng} \cdot \text{cm}^{-2}$ ) as compared to the POx-BBBs grafted on glass. This indicates that the substrate surface is effectively rendered by the POx-BBBs and the Fn adsorption is predominantly affected by the protein/polymer interactions.

In general, we can derive a conclusive picture which is in agreement with the findings on protein adsorption on BBBs: hydrophilic POx side chains of sufficient

length ( $m > 10$ ) provide a very low protein adsorption. Already short BBB pendant chains results in efficient surface chain crowding to render inevitable substrate and layer defects. Side chain end group functionalization were found to have some but not a significant effect upon the protein adsorption. However, also for highly mobile polymer brush surfaces, hydrogen-bonding donors seems to promote protein adsorption to some extent while acceptors such as esters result in good to excellent protein repellency. This opens the possibility to additional surface functionalization of the flexible pendant chains in order to realize biosensing without impairing the protein-repellant properties of the coating. The comparison of POx-BBBs with similar contact angle values but from a different series (e.g., PMeOx, PMeOx2, PMeOx4, and PMeOx-Pip) gives a consistent result concerning Fn adsorption independent from the total polymer layer thickness.

Additional to our protein adsorption screening on to the various POx layers, we examined the initial adhesion of HUVEC to the POx-BBB surfaces. Under physiological conditions, it is generally accepted that the adhesion of cells to a solid surface is mainly mediated by the presence of an adsorbed protein layer, which promotes the attachment and determine the final cellular response. Especially, the high serum concentration and cell-secreted protein ligands

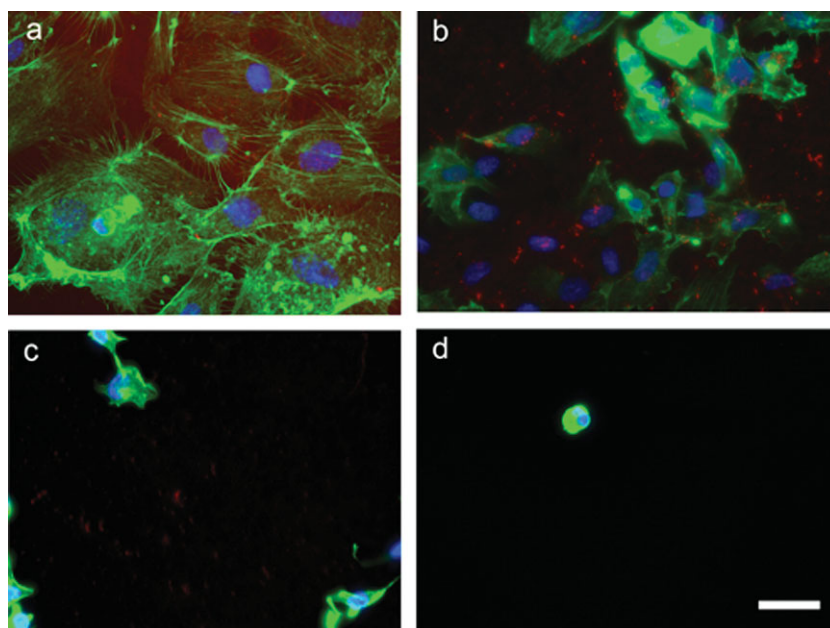


**Figure 5.** Examples of cell adhesion on the different POx-BBBs preexposed to Fn investigated by fluorescence microscopy. In correlation to the amount of adsorbed Fn (see Figure 4), different degrees of cell adhesion can be observed: (a) very good cell adhesion with highly spread cells on PnPrOx with more hydrophobic side chains, (b) reduced cell adhesion with fewer spread cells on PMeOx-Boc, (c) almost suppressed cell adhesion with few and mostly unspread or highly elongated cells on PMeOx-OH, (d) no cell adhesion on protein-repellent PMeOx2<sup>GC</sup>. [Labeling: Fn (red), actin (green), and nuclei (blue). Scale bar: 50  $\mu\text{m}$ ].

have to be considered to adsorb to the materials surface and control cell adhesion. POx-BBB samples after (attempted) Fn adsorption were seeded with HUVEC and cultivated up to 24 h. As initial experiments showed similar adhesion characteristics after 1 h after seeding with the same distinct pattern in comparison to adherent cell density after 24 h, most experiments were performed over 1 h of cell culture only. The samples were fixed and stained and the density and spreading state of cells were evaluated by fluorescence microscopy. As shown in Figure 5a–c, even moderate Fn adsorption resulted in cell adhesion which is evidenced by the density of attached cells and enlarged area due to cell spreading. All surfaces that effectively suppressed Fn adhesion showed no cell adhesion or spreading as exemplarily shown in Figure 5d for the PMeOx<sup>GC</sup> surface. These cell adhesion studies nicely support the results of the Fn adsorption.

An in-depth analysis would require more challenging cell experiments and at best in vivo test series, however, as a first screening test for the performance of POx-BBB with differences in side chain composition and length as well as end group polarity, the presented protein adsorption, and cell adhesion experiments provide a conclusive result.

#### 4. Conclusion

The SIPGP-SI-LCROP approach allows the preparation of POx-BBBs of defined architecture, composition, and chemical functions on various surfaces including carbon or carbonaceous surfaces via direct grafting or oxides by using silane SAMs. Depending on the side chain length and composition, POx-based BBBs can effectively control the protein adsorption behavior and the cell adhesion. For hydrophilic POx-BBBs with PMeOx or PEtOx side chains Fn adsorption was very low ( $\leq 6 \text{ ng} \cdot \text{cm}^{-2}$ ) and thus close to the detection limit. The study shows the non-fouling behavior of hydrophilic POx-BBBs to be comparable to PEG-based coatings of similar molecular architecture. However, since polyethers are prone to oxidative degradation, the non-degradable peptide-like POx polymer might be the better choice if a long-term use within the human body is desired. Since the SIPGP grafting approach is suitable for almost all kinds of substrates including materials of exceptional mechanical strength such as diamond,<sup>[65,87]</sup> silicon carbide,<sup>[88]</sup> graphene,<sup>[89]</sup> and all carbon templated inorganic materials,<sup>[73]</sup> the presented approach have high potential for the development of long-term anti-fouling coatings of implants and functional biosensors.

Acknowledgements: N.Z. is thankful for support by the CompInt (International Graduate School of complex interface) of the TU München through a Ph.D. fellowship. R.J. is thankful for further

support by the IGSSE (International Graduate School for Science and Engineering). R.J. and C.W. acknowledge support by the Center for Regenerative Therapies Dresden (CRTD). R.L. is thankful for a postdoctoral fellowship of the King Abdullah University of Science and Technology (KAUST, Award. No. KUK-F1-029-32). The authors thank Kati Mittasch and Juliane Drichel for technical support in protein adsorption and cell culture experiments.

Received: January 24, 2012; Revised: February 29, 2012; Published online: DOI: 10.1002/mabi.201200026

Keywords: cell adhesion; polymer brushes; polyoxazolines; protein adsorption; surface-initiated polymerization

- [1] E. A. Vogler, *Biomaterials* **2012**, *33*, 1201.
- [2] M. Mrksich, G. M. Whitesides, *Annu. Rev. Biophys. Biomol. Struct.* **1996**, *25*, 55.
- [3] E. Ostuni, R. G. Chapman, R. E. Holmlin, S. Takayama, G. M. Whitesides, *Langmuir* **2001**, *17*, 5605.
- [4] J. E. Raynor, J. R. Capadona, D. M. Collard, T. A. Petrie, A. J. Garcia, *Biointerphases* **2009**, *4*, FA3.
- [5] R. R. Bhat, B. N. Chaney, J. Rowley, A. Liebmman-Vinson, J. Genzer, *Adv. Mater.* **2005**, *17*, 2802.
- [6] K. L. Prime, G. M. Whitesides, *Science* **1991**, *252*, 1164.
- [7] P. Harder, M. Grunze, R. Dahint, G. M. Whitesides, P. E. Laibinis, *J. Phys. Chem. B* **1998**, *102*, 426.
- [8] S. Herrwerth, W. Eck, S. Reinhardt, M. Grunze, *J. Am. Chem. Soc.* **2003**, *125*, 9359.
- [9] A. Hucknall, S. Rangarajan, A. Chilkoti, *Adv. Mater.* **2009**, *21*, 2441.
- [10] H. Ma, J. Hyun, P. Stiller, A. Chilkoti, *Adv. Mater.* **2004**, *16*, 338.
- [11] H. Ma, D. Li, X. Sheng, B. Zhao, A. Chilkoti, *Langmuir* **2006**, *22*, 3751.
- [12] X. Fan, L. Lin, P. B. Messersmith, *Biomacromolecules* **2006**, *7*, 2443.
- [13] J. N. Kizhakkedathu, J. Janzen, Y. Le, R. K. Kainthan, D. E. Brooks, *Langmuir* **2009**, *25*, 3794.
- [14] L. Ionov, A. Synytska, E. Kaul, S. Diez, *Biomacromolecules* **2010**, *11*, 233.
- [15] G. Gunkel, M. Weinhart, T. Becherer, R. Haag, W. T. Huck, *Biomacromolecules* **2011**, *12*, 4169.
- [16] R. Konradi, B. Pidhatika, A. Mühlebach, M. Textor, *Langmuir* **2008**, *24*, 613.
- [17] B. Pidhatika, J. Moller, V. Vogel, R. Konradi, *Chimia* **2008**, *62*, 264.
- [18] S. I. Jeon, J. H. Lee, J. D. Andrade, P. G. De Gennes, *J. Colloid Interface Sci.* **1991**, *142*, 149.
- [19] A. Halperin, *Langmuir* **1999**, *15*, 2525.
- [20] R. A. Latour, *J. Biomed. Mater. Res. A* **2006**, *78*, 843.
- [21] N. Adams, U. S. Schubert, *Adv. Drug Deliv. Rev.* **2007**, *59*, 1504.
- [22] M. Barz, R. Luxenhofer, R. Zentel, M. J. Vicent, *Polym. Chem.* **2011**, *2*, 1900.
- [23] H. Schlaad, C. Diehl, A. Gress, M. Meyer, A. L. Demirel, Y. Nur, A. Bertin, *Macromol. Rapid Commun.* **2010**, *31*, 511.
- [24] K. Knop, R. Hoogenboom, D. Fischer, U. S. Schubert, *Angew. Chem. Int. Ed.* **2010**, *49*, 6288.
- [25] T. X. Viegas, M. D. Bentley, J. M. Harris, Z. Fang, K. Yoon, B. Dizman, R. Weimer, A. Mero, G. Pasut, F. M. Veronese, *Bioconjug. Chem.* **2011**, *22*, 976.
- [26] R. Hoogenboom, *Angew. Chem. Int. Ed.* **2009**, *48*, 7978.

- [27] A. Mero, G. Pasut, L. D. Via, M. W. M. Fijten, U. S. Schubert, R. Hoogenboom, F. M. Veronese, *J. Controlled Release* **2008**, *125*, 87.
- [28] J. Tong, R. Luxenhofer, X. Yi, R. Jordan, A. V. Kabanov, *Mol. Pharm.* **2010**, *7*, 984.
- [29] R. Luxenhofer, G. Sahay, A. Schulz, D. Alakhova, T. K. Bronich, R. Jordan, A. V. Kabanov, *J. Controlled Release* **2011**, *153*, 73.
- [30] R. Luxenhofer, A. Schulz, C. Roques, S. Li, T. K. Bronich, E. V. Batrakova, R. Jordan, A. V. Kabanov, *Biomaterials* **2010**, *31*, 4972.
- [31] M. C. Woodle, C. M. Engbers, S. Zalipsky, *Bioconjugate Chem.* **1994**, *5*, 493.
- [32] D. D. Lasic, D. Needham, *Chem. Rev.* **1995**, *95*, 2601.
- [33] S. Zalipsky, C. B. Hansen, J. M. Oaks, T. M. Allen, *J. Pharm. Sci.* **1996**, *85*, 133.
- [34] M. C. Woodle, *Adv. Drug Deliv. Rev.* **1998**, *32*, 139.
- [35] R. Jordan, K. Martin, H. J. Räder, K. K. Unger, *Macromolecules* **2001**, *34*, 8858.
- [36] A. P. Siegel, M. J. Murcia, M. Johnson, M. Reif, R. Jordan, J. Rühle, C. A. Naumann, *Soft Matter* **2010**, *6*, 2723.
- [37] P. C. Seitz, M. D. Reif, O. V. Konovalov, R. Jordan, *Chem. Phys. Chem.* **2009**, *10*, 2876.
- [38] M. A. Deverall, S. Garg, K. Lütke, R. Jordan, J. Rühle, C. A. Naumann, *Soft Matter* **2008**, *4*, 1899.
- [39] S. Garg, J. Rühle, K. Lütke, R. Jordan, C. A. Naumann, *Biophys. J.* **2007**, *92*, 1263.
- [40] O. Purrucker, A. Förtig, R. Jordan, M. Tanaka, *Chem. Phys. Chem.* **2004**, *5*, 327.
- [41] O. Purrucker, S. Gönnerwein, A. Förtig, R. Jordan, M. Rusp, M. Bärmann, L. Moroder, E. Sackmann, M. Tanaka, *Soft Matter* **2007**, *3*, 333.
- [42] O. Purrucker, A. Förtig, R. Jordan, E. Sackmann, M. Tanaka, *Phys. Rev. Lett.* **2007**, *98*, 078102.
- [43] O. Purrucker, A. Förtig, K. Lütke, R. Jordan, M. Tanaka, *J. Am. Chem. Soc.* **2005**, *127*, 1258.
- [44] F. Rehfeldt, M. Tanaka, L. Pagnoni, R. Jordan, *Langmuir* **2002**, *18*, 4908.
- [45] M. B. Foreman, J. P. Coffman, M. J. Murcia, S. Cesana, R. Jordan, G. S. Smith, C. A. Naumann, *Langmuir* **2003**, *19*, 326.
- [46] D. A. Herold, K. Keil, D. E. Bruns, *Biochem. Pharmacol.* **1989**, *38*, 73.
- [47] M. Shen, L. Martinson, M. S. Wagner, D. G. Castner, B. D. Ratner, T. A. Horbett, *J. Biomater. Sci., Polym. Ed.* **2002**, *13*, 367.
- [48] L. Li, S. Chen, S. Jiang, *J. Biomater. Sci. Polym. Ed.* **2007**, *18*, 1415.
- [49] T. Lehmann, J. Rühle, *Macromol. Symp.* **1999**, *142*, 1.
- [50] H. Wang, L. Li, Q. Tong, M. Yan, *ACS Appl. Mater. Interfaces* **2011**, *3*, 3463.
- [51] J. Kronek, Z. Kroneková, J. Lustoň, E. Paulovičová, L. Paulovičová, B. Mendrek, *J. Mater. Sci. Mater. Med.* **2011**, *22*, 1725.
- [52] F. C. Gaertner, R. Luxenhofer, B. Blechert, R. Jordan, M. Essler, *J. Controlled Release* **2007**, *119*, 291.
- [53] A. R. Statz, J. Kuang, C. Ren, A. E. Barron, I. Szleifer, P. B. Messersmith, *Biointerphases* **2009**, *4*, FA22.
- [54] S. S. Sheiko, B. S. Sumerlin, K. Matyjaszewski, *Prog. Polym. Sci.* **2008**, *33*, 759.
- [55] M. Bernfield, M. Götte, P. W. Park, O. Reizes, M. L. Fitzgerald, J. Lincecum, M. Zako, *Annu. Rev. Biochem.* **1999**, *68*, 729.
- [56] S. H. Kim, J. Turnbull, S. Guimond, *J. Endocrinol.* **2011**, *209*, 139.
- [57] L. Kjellén, U. Lindahl, *Annu. Rev. Biochem.* **1991**, *60*, 443.
- [58] R. V. Iozzo, *Annu. Rev. Biochem.* **1998**, *67*, 609.
- [59] C. Weber, C. R. Becer, R. Hoogenboom, U. S. Schubert, *Macromolecules* **2009**, *42*, 2965.
- [60] C. Weber, C. Remzi Becer, W. Guenther, R. Hoogenboom, U. S. Schubert, *Macromolecules* **2010**, *43*, 160.
- [61] O. Nuyken, J. Rueda-Sanchez, B. Voit, *Polym. Bull.* **1997**, *38*, 657.
- [62] N. Zhang, S. Huber, A. Schulz, R. Luxenhofer, R. Jordan, *Macromolecules* **2009**, *42*, 2215.
- [63] N. Zhang, M. Steenackers, R. Luxenhofer, R. Jordan, *Macromolecules* **2009**, *42*, 5345.
- [64] N. A. Hutter, A. Reitingner, N. Zhang, M. Steenackers, O. A. Williams, J. A. Garrido, R. Jordan, *Phys. Chem. Chem. Phys.* **2010**, *12*, 4360.
- [65] N. A. Hutter, M. Steenackers, A. Reitingner, O. A. Williams, J. A. Garrido, R. Jordan, *Soft Matter* **2011**, *7*, 4861.
- [66] A. Härtl, E. Schrnich, J. A. Garrido, J. Hernando, S. C. Catharino, S. Walter, P. Feulner, A. Kromka, D. Steinmüller, M. Stutzmann, *Nat. Mater.* **2004**, *3*, 736.
- [67] I. Amin, M. Steenackers, N. Zhang, R. Schubel, A. Beyer, A. Götzhäuser, R. Jordan, *Small* **2011**, *7*, 683.
- [68] M. Steenackers, A. Küller, S. Stoycheva, M. Grunze, R. Jordan, *Langmuir* **2009**, *25*, 2225.
- [69] W. Seeliger, E. Aufderhaar, W. Diepers, R. Nehring, W. Thier, H. Hellmann, *Angew. Chem. Int. Ed.* **1966**, *5*, 875.
- [70] S. Huber, R. Jordan, *Colloid Polym. Sci.* **2008**, *286*, 395.
- [71] L. Renner, T. Pompe, K. Salchert, C. Werner, *Langmuir* **2004**, *20*, 2928.
- [72] M. Herklotz, C. Werner, T. Pompe, *Biomaterials* **2009**, *30*, 35.
- [73] M. Steenackers, R. Jordan, A. Küller, M. Grunze, *Adv. Mater.* **2009**, *21*, 2921.
- [74] N. Balachander, C. N. Sukenik, *Langmuir* **1990**, *6*, 1621.
- [75] E. T. Vandenberg, L. Bertilsson, B. Liedberg, K. Uvdal, R. Erlandsson, H. Elwing, I. Lundstrom, *J. Colloid. Interface Sci.* **1991**, *147*, 103.
- [76] J. A. Howarter, J. P. Youngblood, *Langmuir* **2006**, *22*, 11142.
- [77] S. Flink, F. C. J. M. van Veggel, D. N. Reinhoudt, *J. Phys. Org. Chem.* **2001**, *14*, 407.
- [78] R. Jordan, N. West, A. Ulman, Y. M. Chou, O. Nuyken, *Macromolecules* **2001**, *34*, 1606.
- [79] R. Jordan, A. Ulman, *J. Am. Chem. Soc.* **1998**, *120*, 243.
- [80] R. Luxenhofer, M. Bezen, R. Jordan, *Macromol. Rapid Commun.* **2008**, *29*, 1509.
- [81] S. Salzinger, S. Huber, S. Jaksch, P. Busch, R. Jordan, C. M. Papadakis, *Colloid Polym. Sci.* **2012**, *290*, 385.
- [82] J. S. Park, K. Kataoka, *Macromolecules* **2007**, *40*, 3599.
- [83] R. Hoogenboom, H. M. L. Thijs, M. J. H. C. Jochems, B. M. van Lankvelt, M. W. M. Fijten, U. S. Schubert, *Chem. Commun.* **2008**, 5758.
- [84] S. Huber, N. Hutter, R. Jordan, *Colloid Polym. Sci.* **2008**, *286*, 1653.
- [85] N. Zhang, R. Luxenhofer, R. Jordan, *Macromol. Chem. Phys.* **2012**, in print (DOI: 10.1002/macp.201200015).
- [86] T. Pompe, S. Zschoche, N. Herold, K. Salchert, M. F. Gouzy, C. Sperling, C. Werner, *Biomacromolecules* **2003**, *4*, 1072.
- [87] M. Steenackers, S. Q. Lud, M. Niedermeier, P. Bruno, D. M. Gruen, P. Feulner, M. Stutzmann, J. A. Garrido, R. Jordan, *J. Am. Chem. Soc.* **2007**, *129*, 15655.
- [88] M. Steenackers, I. Sharp, K. Larson, N. Hutter, M. Stutzmann, R. Jordan, *Chem. Mater.* **2010**, *22*, 272.
- [89] M. Steenackers, A. M. Gigger, N. Zhang, F. Deubel, M. Seifert, L. H. Hess, C. H. Y. X. Lim, K. P. Loh, J. A. Garrido, R. Jordan, M. Stutzmann, I. D. Sharp, *J. Am. Chem. Soc.* **2011**, *133*, 10490.